Non-Linear Modeling and Sensitive Analysis of a Magnetostrictive Force Sensor

Mojtaba Ghodsi
School of Energy and Electronic Engineering
University of Portsmouth
Portsmouth, UK
e-mail: mojtaba.ghodsi@port.ac.uk

Morteza Mohammadzaheri
Mechanical and Industrial Engineering Department,
Sultan Qaboos University,
Muscat, Oman
e-mail: morteza@squ.edu.om

Payam Soltani
School of Mechanical,
Aerospace and Automatic Engineering
Coventry University, UK
e-mail: payam.soltani@coventry.ac.uk

Abstract— **In this paper, a non-linear model is presented for a magnetostrictive force sensor and the effective parameters in the sensor are highlighted. It was found that pre-stress and bias magnetic fields are the most significant parameters. It was observed that the presented force sensor has linear behavior for an applied force range from 100 to 1700 N. Response Surface Method (RSM) was employed to analyze the sensitivity of the sensor against the effective parameters. It was found that the pre-stress and bias magnetic field and their interactions play a significant role in the sensitivity of the force sensor. Furthermore, it was manifested that the linearity can be enhanced by increasing the pre-stress. On the other hand, the sensitivity of the sensor will be sacrificed by increasing the pre-stress. Bias magnetic field plays the same role. The sensor's sensitivity can be enhanced by increasing the bias magnetic field. Conversely, the sensor loses its linearity in a higher magnetic field. Therefore, there is a trade-off between sensor sensitivity and nonlinearity and both are adjustable by both, pre-stress and magnetic bias.**

Keywords- Force Sensor; Non-Linear Model; Sensitivity; Non-linearity; Pre-steers; Magnetic Bias.

I. INTRODUCTION

Nowadays, the force sensing element is an inevitable feedback element in many control systems in industries. Warning alarms of the seat belt in automobiles, manipulators of robots, and oil/gas monitoring systems are highly dependent on the force/pressure sensing elements. Compared to the traditional force sensors using strain gages, smart materials are promising better static and dynamic characteristics. Piezoelectric elements have been employed as smart sensors for many years [1][2]. However, the piezoelectric element is brittle and its output signal transmission cannot be wireless. On the other hand, a magnetostrictive force sensor has some outstanding merits in comparison with the other force sensors such as machinability [3]-[6], high coupling factor between elastic and magnetic states (about 0.7), heavy loads withstanding [7], adaptive with a harsh environment [8], low response time (about a few microseconds), zero-energy consumption [9] and is suitable for wireless applications [10]. It is required to mention that magnetostrictive materials suffer from some disadvantages such as Hysteresis behavior, Eddy current loss, and thermal instability. Talebian presented a good enough model for Hysteresis [11] and Eddy current loss [12]. Furthermore, Ghodsi et al. employed a thermoelectric cooler to remove heat generated by the excitation coil [13][14]. Magnetostrictive force sensors are based on the Villari effect [15]. Therefore, when subjected to a mechanical force, their magnetization varies and we can measure the variation of magnetic field density passing through the magnetostrictive bar. This variation can be proportional to the applied mechanical load. Calkins et al. and Stachowiak investigated the effects of pre-stress on the dynamic performance of Terfenol-D transducers/actuators [16][17]. Many researchers developed various types of magnetostrictive force sensors. Zhu et al. proposed a model for a giant magnetostrictive force sensor and investigated the effect of frequency on the output voltage of the sensor [18]. A precise impact force sensor using Galfenol has been developed by Shu et al. They showed that the cantilever type is more sensitive than the rod type [19]. Galfenol was employed to develop a high sensitivity and linearity tactile magnetostrictive force sensor in 2019 [20]. Despite high linearity, this cantilever force sensor is suitable for a low range of force detection less than 5 N.

In this paper, after presenting the principle of the sensor in Section 2, a non-linear magneto-mechanical model for giant magnetostrictive force is combined with Faraday's law to predict the generated voltage by a search coil. Furthermore, the sensitive analysis of the sensor and the effects of parameters on the sensor's performance will be discussed in Section 3.

 ISBN: 978-1-61208-766-5

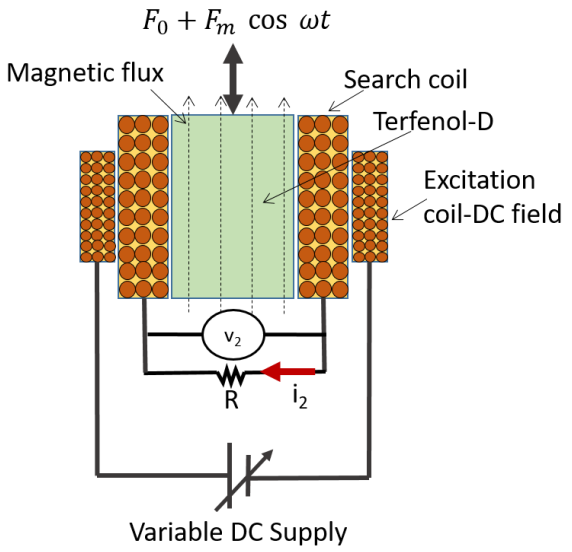

Figure1. Schematic of the force sensor

II. PRINCIPLE AND MODELING OF FORCE SENSOR

A. Principle of Operation

The proposed force sensor consists of a core made of Giant Magnetostrictive Material (GMM) which is in the presence of a bias magnetic field, a search coil, and an excitation coil to generate a bias magnetic field (Figure 1). The bias magnetic field can be generated by permanent magnets or a coil energized by a variable DC power supply. Applied force changes the magnetic flux density pass through the Terfenol-D. Based on Faraday's law, the variation of magnetic flux can be detected by the generated voltage across the resistive load connected to the ends of the search coil. The amplitude of the generated voltage (V_2) is proportional to the amplitude of the applied force (F_m). The proportional relationship can be changed to an equal relationship by (1).

$$V_2 = k\,(H_0, F_0)\,F_m \tag{1}$$

k is the coefficient, which is dependent on the magnetic bias and pre-stress applied to the Terfenol-D. The effect of magnetic bias and pre-stress will be examined in the next section.

B. Non-linear Analytical Modeling

This section aims to find a relationship between the amplitude of the applied force and the amplitude of the induced voltage. By applying axial harmonic force consists of bias force to the magnetostrictive bar, Terfenol-D, the sensitive part of the sensor is subjected to tensile and compressive normal stresses. By assuming the vibration as the axial harmonic force, the non-linear magneto-mechanical relation of Terfenol-D can be presented in (2) [21].

$$\begin{cases} \varepsilon = \dfrac{\sigma}{E} - \dfrac{M_s}{\gamma}\left[\dfrac{\gamma H}{\sigma}\tanh\left(\dfrac{\gamma H}{\sigma}\right) - \ln\left(\cosh\left(\dfrac{\gamma H}{\sigma}\right)\right)\right] \\ B = \mu_0 H + M_s \tanh\left(\dfrac{\gamma H}{\sigma}\right) \end{cases} \tag{2}$$

where B is magnetic flux density, H is the magnetic field ε , and σ are strain and the applied stress, respectively. For Terfenol-D, the best value of γ and M_s are -347 and 0.8, respectively [12][22]. The magnetic field consists of two components of (a) magnetic field bias, H_0, (b) magnetic field caused by generated current, $\widehat{H}$. Using Ampere's law, the magnetic field can be concluded as (3).

$$H = H_0 + \widehat{H} = H_0 + \frac{N i_2}{l_0} \tag{3}$$

where N is the number of turns of the search coil, i_2 is induced current due to the applied force and l_0 is the length of the Terfenol-D bar. Based on Faraday's law, the relationship between magnetic flux and generated voltage can be written as follow:

$$\varphi = BA = -\frac{1}{N}\int v_2\,dt \tag{4}$$

By substituting (3) and (4) into (2) and considering $F=\sigma A$ and $v_2=Ri_2$ the induced current can be derived by solving differential (5).

$$-\frac{R}{L_0}\int_0^{\tau} i_2\,dt = i_2 + \frac{NAM_s}{L_0}\tanh\left(\frac{\frac{\gamma A N i_2}{l_0} + \gamma A H_0}{F_0 + F_m\cos\omega t}\right) + \frac{NA\mu_0}{L_0}H_0 \tag{5}$$

To solve this non-linear differential equation, we employed the Simulink of MATLAB (Appendix A). The parameters of the force sensor are shown in Table I. The sample of output voltage calculated by Simulink is shown in Figure 2 while the sensor is under harmonic force. Figure 3 shows the simulated relationship between applied force and output voltage when the magnetostrictive force sensor is under various magnetic fields from 100 to 20 kA/m, and constant bias compressive force is about 1000 N. It is obvious that the force sensor has a linear behavior in the range from 100 to 1700 N. Furthermore, magnetic bias has a positive effect on the sensitivity of the sensor while its nonlinearity is magnified for force amplitude larger than 1700 N. The effect of bias force (pre-stress) is simulated in Figure 4. It is found that higher pre-stress causes lower sensitivity. However, pre-stress is helpful to enhance the linearity of the sensor in a force range higher than 1700 N.

 ISBN: 978-1-61208-766-5

TABLE I. FORCE SENSOR PARAMETERS

Terms	Values
Cross-section of Terfenol-D, *A*	78.5 (mm^2)
Young Modulus, *E*	45 (GPa)
Terfenol-D density, ρ	9200 (kg/m^3)
External Resistor	0.3 Ω
Number of turns in pickup coil, *N*	300
Length of the Terfenol-D and search coil, l_0	50 (mm)
Relative magnetic permeability, μ_r	12-25

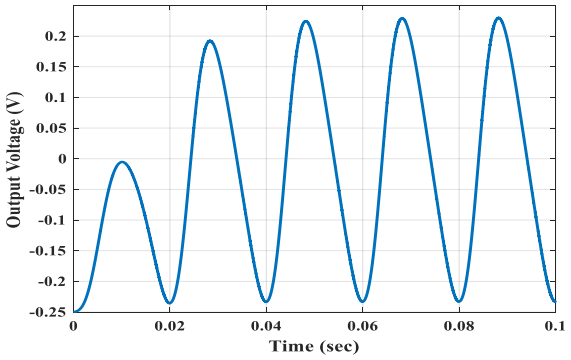

Figure 2. Output voltage of search coil, , R=0.3 Ω, H_0=5 kA/m, F_0= -1060 N, F_m= 1000 N, f= 50 Hz (simulated results)

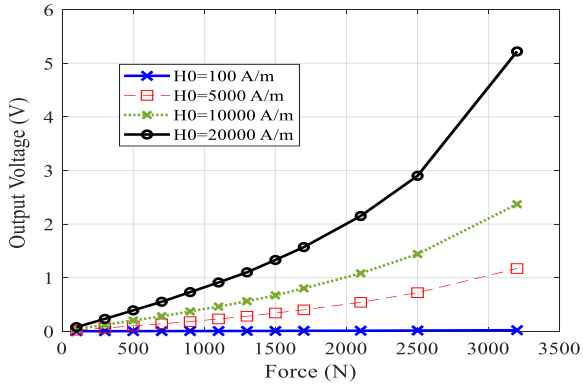

Figure 3. Output voltage of force sensor (V_{pp}); R=0.3 Ω ; F_0 = -1000 N (simulated results)

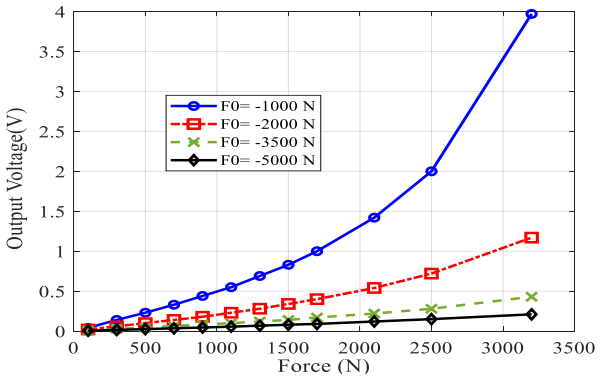

Figure 4. Output voltage of force sensor (V_{pp}); R=0.3 Ω ; H_0 = 5000 A/m (simulated results)

III. SENSITIVITY ANALYSIS OF THE FORCE SENSOR

Referring to the (5), and the sample of the voltage output shown in Figures 2 to 4, the magnetic bias and pre-stress seem to be effective on the measured voltage across the search coil. To examine this assumption, the Design Of Experiments (DOE) was exploited [23][24]. The goal of this part is to determine the optimum operating conditions while the pre-stress and bias magnetic fields are assumed adjustable. The variable factors in this force sensor are F_0 and H_0. To maximize the output voltage, the Response Surface Method (RSM) is employed to find proper values for each factor to have optimum output voltage [25][26]. To specify a regression equation between the amplitude of output voltage and pre-stress and magnetic bias, Minitab 17 software is used. Table II shows two factors with five levels for each. Based on the design proposed by RSM and selection of $\alpha = 1.44$, it is found that nine simulation results including one center point are required (Table III). Table IV shows the P_{value} and the coefficients of each factor. Since the P_{value} of $H_0 \times H_0$ is greater than 0.05, the effect of this term, $H_0 \times H_0$, is ignorable on the output voltage. However, F_0, H_0, and their interaction are effective, since their P_{value} is smaller than 0.05. R-Sq = 98.38% shows the goodness of the model represented by RSM.

TABLE II. CODED INPUT VARIABLES

Factors	- α	-1	0	1	+ α
F_0	-3940	-3500	-2500	-1500	-1060
H_0	1400	2500	5000	7500	8600

TABLE III. ANALYTICAL RESULTS USED IN RSM

Order	F_0 (N)	H_o (A/m)	V_m (v)
1	-3500	2500	0.023
2	-1500	2500	0.075
3	-3500	7500	0.07
4	-1500	7500	0.225
5	-3940	5000	0.038
6	-1060	5000	0.23
7	-2500	1400	0.0215
8	-2500	8600	0.13
9	-2500	5000	0.075

TABLE IV. COEFFICIENT OF REGRESSION EQUATION AND P_{VALUE} IN INITIAL AND MODIFIED MODELS

Terms	Initial Model		Modified Model	
	Reg. Eq. Coefficient	P_{value}	Reg. Eq. Coefficient	P_{value}
Constant	0.075	0.00	0.07411	0.00
F_0	0.5982	0.00	0.05982	0.00
H_0	0.04381	0.00	0.04381	0.00
$F_0 \times H_0$	0.02575	0.002	0.02575	0.001
$F_0 \times F_0$	0.02784	0.000	0.02801	0.000
$H_0 \times H_0$	-0.00128	0.767	---------	------

 ISBN: 978-1-61208-766-5

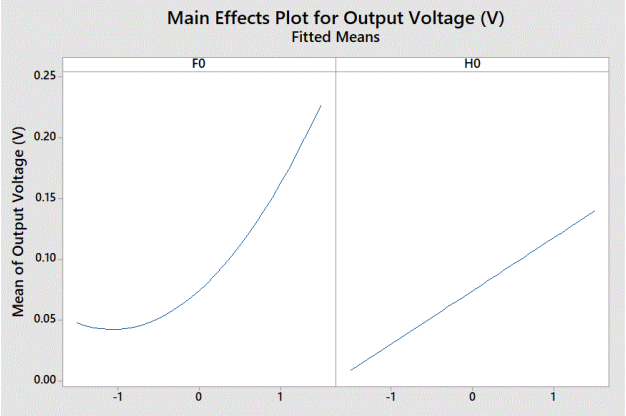

Figure 5. Relationship between the output voltage and main effects, F_0 and H_0

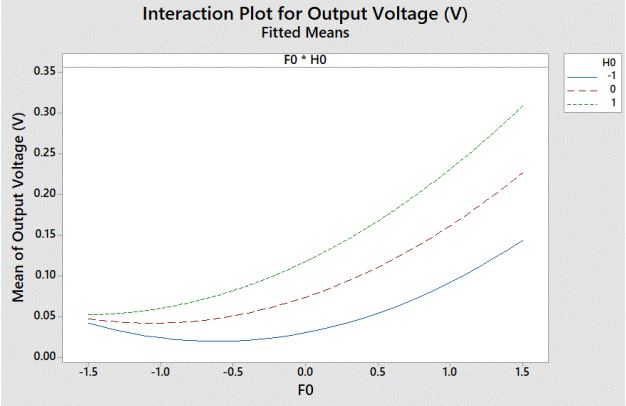

Figure 6. Interaction between F_0 and H_0

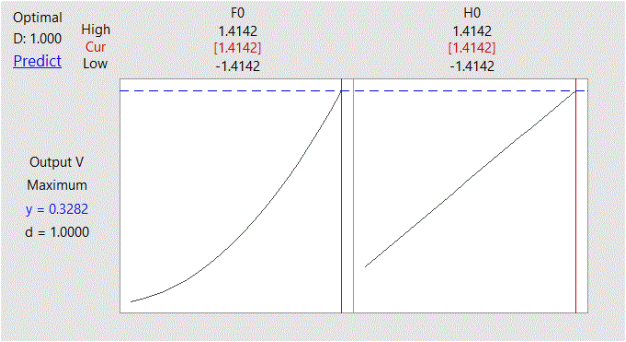

Figure 7. RSM optimizer to predict the maximum output

Based on the coefficients presented in Table IV, the output voltage can be modeled by (6):

$$V_2(v) = 0.07411 + 0.05982\,F_0 + 0.04381\,H_0 + 0.02801\,F_0 \times F_0 + 0.02575\,F_0 \times H_0 \quad (6)$$

Therefore, among the factors and their interactions, F_0 has the highest effect since its coefficient is the largest. Figures 5 and 6 show the main effects and interactions between the main factors. One of the biggest advantages of RSM is determining the maximum output voltage. Figure 7 predicts that the maximum amplitude of output voltage (V_m) can be enhanced to 0.32 V, when both F_0 and H_0 are 1060 N and 8.6 kA/m, respectively. This prediction is confirmed when these values are substituted in (5) and the amplitude of output voltage (V_m) reaches 0.4 V.

IV. CONCLUSION

A magnetostrictive force sensor was modeled using non-linear magneto-mechanical coupling equations. The effect of the pre-stress and bias magnetic field was investigated on the sensitivity and nonlinearity of the force sensors. It was highlighted that the presented applied force has linear behavior for the applied force range from 100 to 1700 N. Response Surface Method (RSM) was employed to analyze the sensitivity of the sensor against the effective parameters. It was found that the pre-stress and bias magnetic fields and their interactions play a significant role in the sensitivity of the force sensor. Furthermore, it was manifested that the linearity can be enhanced by increasing the pre-stress. On the other hand, the sensitivity of the sensor will be sacrificed by increasing the pre-stress. Bias magnetic field plays the same role. The sensor's sensitivity can be enhanced by increasing the bias magnetic field. Conversely, the sensor loses its linearity in a higher magnetic field. Consequently, there is a trade-off between sensor sensitivity and nonlinearity and both are adjustable by both, pre-stress and magnetic bias.

REFERENCES

[1] H. Hoshyarmanesh, A. Abbasi, P. Moein, M. Ghodsi, and K. Zareinia, "Design and Implementation of an Accurate, Portable, and Time-Efficient Impedance-Based Transceiver for Structural Health Monitoring," *IEEE/ASME Transactions on Mechatronics*, vol. 22, pp. 2809-2814, 2017.

[2] H. Hoshyarmanesh, M. Ghodsi, M. Kim, H. H. Cho, and H.-H. Park, "Temperature Effects on Electromechanical Response of Deposited Piezoelectric Sensors Used in Structural Health Monitoring of Aerospace Structures," *Sensors*, vol. 19, p. 2805, 2019.

[3] M. Ghodsi, T. Ueno, and T. Higuchi, "Novel Magnetostrictive Bimetal Actuator Using Permendur," *Advanced Materials Research*, vol. 47-50, pp. 262-265, 2008.

[4] A. Saleem, M. Ghodsi, M. Mesbah, and A. Ozer, "Model identification of terfenol-D magnetostrictive actuator for precise positioning control," in *Active and Passive Smart Structures and Integrated Systems 2016*, 2016, p. 97992J.

[5] M. Sheykholeslami, Y. Hojjat, M. Ghodsi, M. Zeighami, and K. Kakavand, "Effect of magnetic field on mechanical properties in Permendur," *Materials Science and Engineering: A*, vol. 651, pp. 598-603, 2016.

[6] M. R. Sheykholeslami, Y. Hojjat, S. Cinquemani, M. Ghodsi, and M. Karafi, "An approach to design and fabrication of resonant giant magnetostrictive transducer," *Smart Structures and Systems*, vol. 17, pp. 313-325, 2016.

[7] M. Ghodsi, S. Mirzamohamadi, S. Talebian, Y. Hojjat, and M. Sheikhi, "Analytical, numerical and experimental investigation of a giant magnetostrictive (GM) force sensor," *Sensor Review*, vol. 35, pp. 357-365, 2015.

[8] M. Ghodsi and M. Modabberifar, "Quality factor, static and dynamic responses of miniature galfenol actuator at wide range of temperature," *International Journal of Physical Sciences*, vol. 6, pp. 8143-8150, 2011.

 ISBN: 978-1-61208-766-5

[9] M. Ghodsi, T. Ueno, H. Teshima, H. Hirano, T. Higuchi, and E. Summers, ""Zero-power" positioning actuator for cryogenic environments by combining magnetostrictive bimetal and HTS," *Sensors and Actuators A: Physical*, vol. 135, pp. 787-791, 2007.

[10] N. Adelsberg, Y. Weber, A. Yoffe, and D. Shilo, "Wireless thin layer force sensor based on a magnetostrictive composite material," *Smart Materials and Structures*, vol. 26, p. 065013, 2017.

[11] S. Talebian, Y. Hojjat, M. Ghodsi, M. R. Karafi, and S. Mirzamohammadi, "A combined Preisach–Hyperbolic Tangent model for magnetic hysteresis of Terfenol-D," *Journal of Magnetism Magnetic Materials*, vol. 396, pp. 38-47, 2015.

[12] S. Talebian, Y. Hojjat, M. Ghodsi, and M. R. Karafi, "Study on classical and excess eddy currents losses of Terfenol-D," *Journal of Magnetism and Magnetic Materials*, vol. 388, pp. 150-159, 2015.

[13] M. Ahanpanjeh, M. Ghodsi, and Y. Hojjat, "Precise Positioning of Terfenol-D Actuator Eliminiating the Heat Generated by Coil," *Modern Applied Science*, vol. 10, pp. 232-244, 2016.

[14] M. Ghodsi, A. Saleem, A. Özer, I. Bahadur, K. Alam, A. Al-Yahmadi, *et al.*, "Elimination of thermal instability in precise positioning of Galfenol actuators," in *Behavior and Mechanics of Multifunctional Materials and Composites 2016*, 2016, p. 980008.

[15] M. Ghodsi, H. Ziaiefar, M. Mohammadzaheri, and A. Al-Yahmedi, "Modeling and Characterization of Permendur Cantilever Beam for Energy Harvesting," *Energy*, vol. 176, pp. 561-569, 2019.

[16] F. T. Calkins, M. J. Dapino, and A. B. Flatau, "Effect of prestress on the dynamic performace of a Terfenol-D transducer," in *Smart Structures and Materials 1997: Smart Structures and Integrated Systems*, 1997, pp. 293-304.

[17] D. Stachowiak, "The influence of magnetic bias and prestress on magnetostriction characteristics of a giant magnetostrictive actuator," *Przegląd Elektrotechniczny,* vol. 89, pp. 233-236, 2013.

[18] Z. Zhu, F. Liu, X. Zhu, H. Wang, and J. Xu, "Vibration analysis and experiment of giant magnetostrictive force sensor," *IOP Conference Series: Materials Science and Engineering*, vol. 274, p. 012071, 2017.

[19] L. Shu, J. Yang, B. Li, Z. Deng, and M. J. Dapino, "Impact force sensing with magnetostrictive Fe-Ga alloys," *Mechanical Systems and Signal Processing*, vol. 139, p. 106418, 2020.

[20] Y. Li, B. Wang, Y. Li, B. Zhang, L. Weng, W. Huang, *et al.*, "Design and output characteristics of magnetostrictive tactile sensor for detecting force and stiffness of manipulated objects," *IEEE Transactions on Industrial Informatics*, vol. 15, pp. 1219-1225, 2018.

[21] C. S. Clemente and D. Davino, "Modeling and characterization of a kinetic energy harvesting device based on galfenol," *Materials*, vol. 12, p. 3199, 2019.

[22] S. Talebian, Y. Hojjat, M. Ghodsi, S. Mirzamoha, and S. Mirzamohammadi, "Study of effects of bias magnetic field and mechanical pre-stress on sensitivity and linear measurement range of Terfonel-D force sensor," *Modares Mechanical Engineering* vol. 13, pp. 46-55, 2013.

[23] M. Ghodsi, "Optimization of mover acceleration in DC tubular linear direct-drive machine using response surface method," *International Review of Electrical Engineering*, vol. 10, pp. 492-500, 2015.

[24] M. Ghodsi, H. Ziaiefar, M. Mohammadzaheri, F. K. Omar, and I. Bahadur, "Dynamic analysis and performance optimization of permendur cantilevered energy harvester," *Smart Structures and Systems*, vol. 23, pp. 421-428, 2019.

[25] M. Ghodsi, H. Ziaifar, M. Mohammadzaheri, and P. Soltani, "Effect of Damping on Performance of Magnetostrictive Vibration Energy Harvester," *International Journal of Mechanical and Mechatronics Engineering*, vol. 14, pp. 147-151, 2020.

[26] M. Ghodsi, H. Ziaifar, M. M. Mohammadzaheri, and P. Soltani, "Effect of inductance ratio on operating frequencies of a hybrid resonant inverter," *International Journal of Energy and Power Engineering*, vol. 14, pp. 123-128, 2020.

 ISBN: 978-1-61208-766-5

Appendix A

Figure A1 shows the Simulink program used to solve the (5).

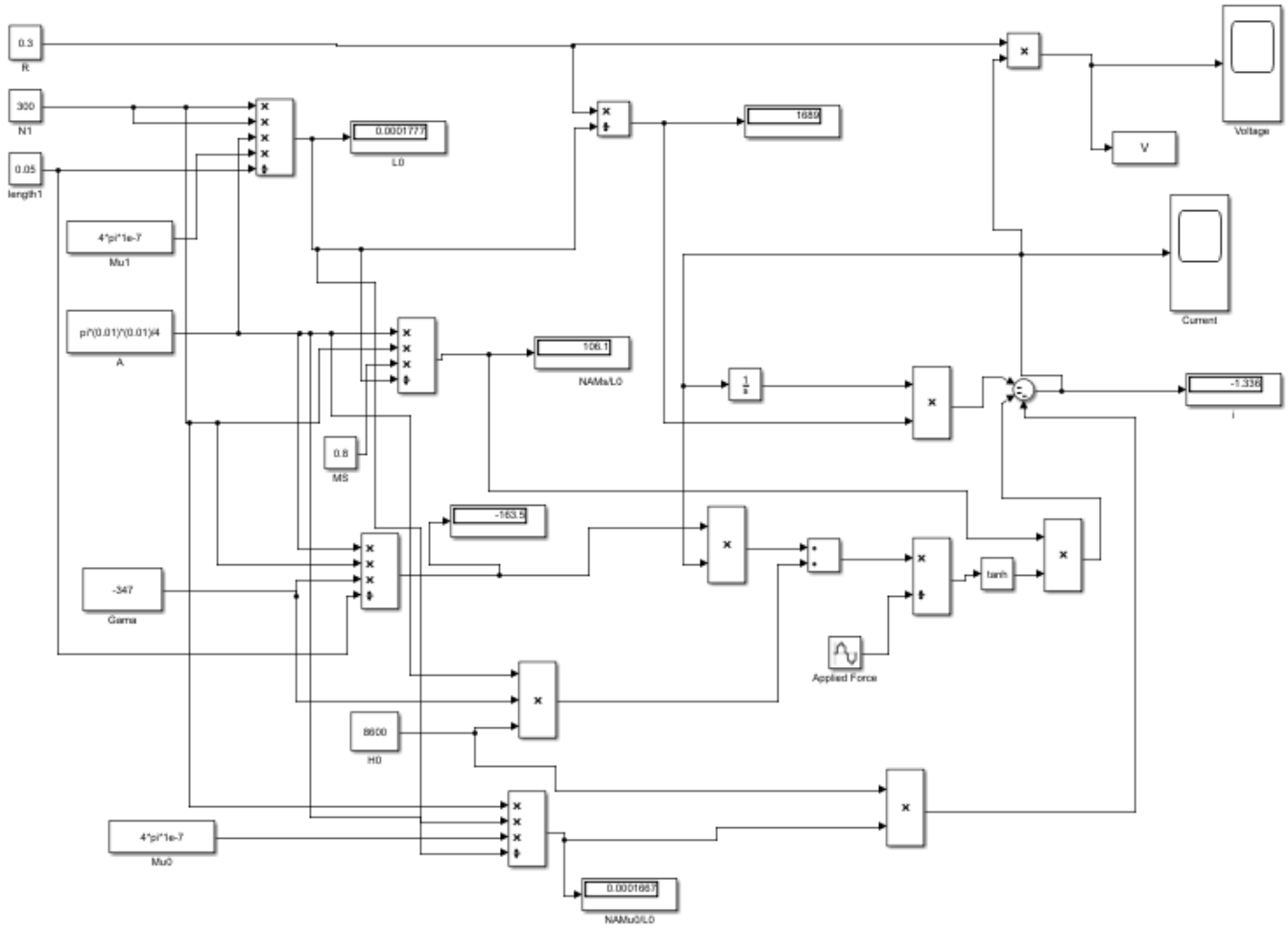

Figure A1. Simulink program to calculate the output voltage